

**Evaluation of a
photosynthesis-
based biogenic
isoprene emission**

F. Pacifico et al.

[Title Page](#)[Abstract](#)[Introduction](#)[Conclusions](#)[References](#)[Tables](#)[Figures](#)[Back](#)[Close](#)[Full Screen / Esc](#)[Printer-friendly Version](#)[Interactive Discussion](#)

⁸DePaul University, Environmental Science Program, Chicago, IL 60614, USA

⁹Department of Atmospheric and Oceanic Sciences, School of Physics, Peking University Beijing, China

¹⁰Department of Environmental Science, Policy, and Management, University of California at Berkeley, Berkeley CA 94720, USA

¹¹Institute of Atmospheric Physics, Chinese Academy of Sciences, Beijing 100029, China

*now at: EOS Group, Department of Physics & Astronomy, University of Leicester, UK

Received: 16 September 2010 – Accepted: 5 November 2010 – Published: 18 November 2010

Correspondence to: F. Pacifico (federica.pacifico@metoffice.gov.uk)

Published by Copernicus Publications on behalf of the European Geosciences Union.

Abstract

We have incorporated a semi-mechanistic isoprene emission module into the JULES land-surface scheme. We evaluate the coupled model against local above-canopy isoprene emission flux measurements from six flux tower sites as well as satellite-derived estimates of isoprene emission over tropical South America and east and south Asia. The model simulates diurnal variability well: correlation coefficients are significant (at the 95% level) for all flux tower sites. The model reproduces day-to-day variability with significant correlations (at the 95% confidence level) at four of the six flux tower sites. At the UMBS site, a complete set of seasonal observations is available for two years (2000 and 2002). The model reproduces the seasonal pattern of emission during 2002, but does less well in the year 2000. Comparison with the satellite-derived isoprene-emission estimates suggests that the model simulates the main spatial patterns, seasonal and inter-annual variability over tropical regions. The model yields a global annual isoprene emission during the 1990s of $380 \pm 7 \text{ TgC yr}^{-1}$.

1 Introduction

Isoprene (C_5H_8) is quantitatively the most important of the non-methane biogenic volatile organic compounds (BVOCs) emitted into the atmosphere (Pacifico et al., 2009). Terrestrial vegetation is the main source (Guenther et al., 2006), although not all plants emit isoprene (Harley et al., 1999; Kesselmeier and Staudt, 1999). Tropical broadleaf trees are considered the main contributors to global isoprene emissions (Guenther et al., 2006). Isoprene is a carbon-containing compound and – after oxidation in the atmosphere – a carbon dioxide (CO_2) precursor, so it is a potentially significant term in the global carbon cycle (Guenther et al., 2002). Isoprene also modulates tropospheric ozone (O_3) and methane (CH_4) concentrations (Hofzumahaus et al., 2009) and is a source of secondary organic aerosol (SOA; Claeys et al., 2004), which affects cloud properties and the surface radiation budget.

Evaluation of a photosynthesis-based biogenic isoprene emission

F. Pacifico et al.

Title Page

Abstract

Introduction

Conclusions

References

Tables

Figures

⏪

⏩

◀

▶

Back

Close

Full Screen / Esc

Printer-friendly Version

Interactive Discussion



**Evaluation of a
photosynthesis-
based biogenic
isoprene emission**

F. Pacifico et al.

Title Page

Abstract

Introduction

Conclusions

References

Tables

Figures



Back

Close

Full Screen / Esc

Printer-friendly Version

Interactive Discussion



Vegetation species composition determines overall emission capacity (Niinemets et al., 2010a, b), but the main environmental controls on isoprene emissions are light (e.g., Monson and Fall, 1989), temperature (e.g., Guenther et al., 1993), atmospheric CO₂ concentration (e.g., Monson et al., 2007) and drought (e.g., Pegoraro et al., 2004; Monson et al., 2007). In the short-term, isoprene emission increases with light and falls to near zero almost immediately after the cessation of illumination. Isoprene emission increases with temperature until a temperature optimum of ca. 40 °C (Niinemets et al., 1999). Moreover, measurements have demonstrated that high concentrations of CO₂ inhibit isoprene emission, but with potentially different response patterns to short- and long-term changes in the CO₂ burden (see summary of studies in Young et al., 2009 and Pacifico et al., 2009). From the limited number of observational and laboratory studies it appears that isoprene emissions are not immediately affected by mild water stress, even when this stress is already affecting photosynthesis (e.g., Sharkey and Loreto, 1993), but the onset of more severe drought causes isoprene emissions to decline substantially (e.g., Pegoraro et al., 2004; Monson et al., 2007). The strong dependence of isoprene emissions on temperature means that isoprene emissions are likely to increase under future climate conditions, although such an increase may be offset by the inhibition of leaf isoprene production emissions that is observed at higher levels of CO₂ (Arneth et al., 2007a). Research on quantifying how isoprene emissions will change (and the magnitude of potential feedbacks on atmospheric chemistry and climate) is still in its infancy (see summary of studies in Pacifico et al., 2009).

Biogenic isoprene emissions were originally modelled using empirical relationships between specific environmental controls and emissions, applying a number of algorithms for the short- and long-term influence of changing environmental conditions (Guenther et al., 1991, 1993, 1995, 2006). More recently, photosynthesis-based schemes have been developed that seek to relate isoprene emission to substrate production mechanistically (Niinemets et al., 1999; Martin et al., 2000; Zimmer et al., 2003; Arneth et al., 2007b). Of these semi-mechanistic models, the Arneth et al. (2007b) scheme is the only one that includes the atmospheric CO₂ inhibition of

isoprene emission, albeit in an empirical form. The scheme has already been coupled to the Lund Potsdam Jena Dynamic Global Vegetation Model (LPJ-DGVM) (Sitch et al., 2003) and to the Lund Potsdam Jena General Ecosystem Simulator (LPJ-GUESS; Smith et al., 2001), and applied at both regional (Arneth et al., 2008b) and global (Arneth et al., 2007a) scales. In this paper, we describe the validation of a modified version of the Arneth et al. (2007b) scheme that has been implemented in the Joint UK Land Environmental Simulator (JULES; Essery et al., 2003; Cox et al., 1998, 1999; www.jchmr.org/jules). The isoprene scheme has been implemented in the land-surface component of the Hadley Centre Global Environmental Model with Earth System component (HadGEM2-ES) and a version of JULES including isoprene will be the land-surface component of the new Hadley Centre Global Environmental Model (HadGEM3), thus the work described here is designed to evaluate model performance prior to quantifying the feedbacks between biogenic emissions, atmospheric chemistry and climate within a global Earth System model (e.g., Arneth et al., 2010).

2 Methods

We have incorporated the isoprene emission scheme described in Arneth et al. (2007b) into the framework of the JULES land-surface model. Here, we first describe the most important features of JULES, we then outline the original isoprene emission scheme, before describing the necessary modifications made to couple the two components. We go on to describe our strategy for the evaluation of the coupled scheme under modern climate conditions (various time periods from 1995 to 2004). Finally, we describe the protocol for a global simulation of isoprene emissions under modern conditions (1990 to 1999).

Evaluation of a photosynthesis-based biogenic isoprene emission

F. Pacifico et al.

Title Page

Abstract

Introduction

Conclusions

References

Tables

Figures



Back

Close

Full Screen / Esc

Printer-friendly Version

Interactive Discussion



2.1 The JULES land-surface scheme

JULES is a UK community land-surface model, based on the MOSES2 (Met Office Surface Exchange Scheme version 2; Essery et al., 2003) land surface scheme used in the UK Met Office Hadley Centre climate model HadGEM (Johns et al., 2006). JULES is intended to replace MOSES in HadGEM3. JULES can be run at a single point or in gridded mode for any number of grid boxes, with a typical time step of 30 to 60 min. The meteorological data used to run JULES are: downward longwave radiation, downward shortwave radiation, precipitation, air pressure, specific humidity, air temperature, and wind speed. These data need to have sub-daily resolution and can be interpolated by JULES itself to the appropriate model time step if necessary. JULES has five plant-functional types (PFTs), namely broadleaf trees, needleleaf trees, C3 grass, C4 grass, and shrubs, and uses a further four surface types (urban, inland water, bare soil and ice). Each gridbox can consist of a number of vegetation and surface types. JULES simulates vegetation dynamics using the TRIFFID DGVM (Cox et al., 2000; Cox, 2001). The photosynthesis modules for C3 and C4 plants are based on the work of Collatz et al. (1991) and Collatz et al. (1992), respectively. A comprehensive description of the JULES photosynthesis scheme is given in Cox et al. (1998). The rate of gross photosynthesis is calculated as the minimum of three limiting factors: the Rubisco-limited rate of gross photosynthesis, the light-limited rate of gross photosynthesis, and the limitation associated with transport of photosynthetic products for C3 plants and PEP-Carboxylase limitation for C4 grasses. Photosynthetically active radiation (PAR) and leaf nitrogen are assumed to decrease exponentially through the canopy (Sellers et al., 1992; Mercado et al., 2007). Canopy photosynthesis is calculated as the sum over all canopy layers (10 layers were used in this study). Leaf phenology is updated on a daily basis, using accumulated temperature-dependent leaf turnover rates. The ability of JULES to simulate photosynthesis has been tested in recent model benchmarking studies, including at ten eddy correlation sites covering the major biomes of the globe (Blyth et al., 2010a, b) and at regional and global scales, using atmospheric

Evaluation of a photosynthesis-based biogenic isoprene emission

F. Pacifico et al.

Title Page

Abstract

Introduction

Conclusions

References

Tables

Figures



Back

Close

Full Screen / Esc

Printer-friendly Version

Interactive Discussion



CO₂ measurements (Cadule et al., 2010; Blyth et al., 2010a, b). Blyth et al. (2010a, b) demonstrates the satisfactory performance of JULES in simulating concurrently the terrestrial carbon and water cycles.

2.2 Isoprene emission scheme

The Arneth et al. (2007b) isoprene emission scheme is based on the biochemical model for isoprene emission developed by Niinemets et al. (1999). In the Niinemets et al. (1999) model, isoprene emission depends on the electron requirement for isoprene synthesis. The model assumes that all isoprene emitted from plant leaves is synthesized in the chloroplasts via the 1-deoxy-xylulose-5-phosphate (DXP) pathway and that a certain proportion of electrons released by PSII (Photosystem II) is used in isoprene synthesis. This proportion is calculated from the estimated energy and redox-equivalents requirements to reduce isoprene from the initial steps of carbon assimilation, considering the requirements of 6 moles assimilated CO₂ for one mole of isoprene produced. The assumption that co-enzymes, rather than carbon precursors, are the rate-limiting step has been shown to reproduce the correct response of isoprene emission to light and temperature under present-day conditions (Niinemets et al., 1999; Arneth et al., 2007b). However, the effects of changing CO₂ concentration, which has been hypothetically linked to competition for carbon substrate (Rosenstiel et al., 2004), need to be included empirically (Arneth et al., 2007b).

When the rate of regeneration of ribulose 1,5-bisphosphate (RuBP) through electron transport is limiting, photosynthetic electron transport (J) is (Farquhar et al, 1980):

$$J = \frac{(A_J + R_D)(4C_1 + 8\Gamma)}{C_1 - \Gamma} \quad (1)$$

where A_J is leaf level net photosynthesis when RuBP is limiting; R_D is leaf level dark respiration; C_1 is leaf internal CO₂ concentration and Γ is photorespiration compensation point.

Evaluation of a photosynthesis-based biogenic isoprene emission

F. Pacifico et al.

Title Page

Abstract

Introduction

Conclusions

References

Tables

Figures

⏪

⏩

◀

▶

Back

Close

Full Screen / Esc

Printer-friendly Version

Interactive Discussion



Based on the co-enzyme and energetic requirements for isoprene synthesis, Niinemets et al. (1999) assume that isoprene emission is nicotinamide adenine dinucleotide phosphate (NADPH) limited. Given that the NADPH requirement per CO₂ mole assimilated is 1.17 times higher for isoprene synthesis than for sugar synthesis and that for each isoprene molecule released 6 CO₂ molecules must be assimilated, the rate of photosynthetic electron transport to sustain isoprene synthesis and emission at the leaf level (I_l) is:

$$J_{\text{isoprene}} = \frac{6I_l(4.67C_1 + 9.33\Gamma)}{C_1 - \Gamma} \quad (2)$$

So

$$I_l = \varepsilon \frac{(A_J + R_D)(4C_1 + 8\Gamma)}{6(4.67C_1 + 9.33\Gamma)} \quad (3)$$

$$\text{where } \varepsilon = \frac{J_{\text{isoprene}}}{J_T} \approx \text{as } J_T = J + J_e \approx J \quad (4)$$

The inhibition of isoprene emission with increasing atmospheric CO₂ concentration is empirically modelled by Arneth et al. (2007b) as:

$$f_{\text{CO}_2} = \frac{C_{1\text{st}}}{C_1} \quad (5)$$

where $C_{1\text{st}}$ is leaf internal CO₂ concentration in standard conditions (i.e. temperature $T_{\text{st}} = 30^\circ\text{C}$ and photosynthetically active radiation $1000 \mu\text{mol m}^{-2} \text{s}^{-1}$) at 370 ppm CO₂ atmospheric concentration. While for the simulation of changes in the long-term CO₂ growth environment C_1 under non-water stressed conditions is applied, in principle, the calculation of f_{CO_2} could also implicitly include the short-term response of isoprene emission to drought stress (Monson et al., 2007). During periods of water limitation,

Evaluation of a photosynthesis-based biogenic isoprene emission

F. Pacifico et al.

Title Page

Abstract

Introduction

Conclusions

References

Tables

Figures

⏪

⏩

◀

▶

Back

Close

Full Screen / Esc

Printer-friendly Version

Interactive Discussion

JULES simulates a closure of stomata, thus C_1 decreases and therefore f_{CO_2} and consequently isoprene emission increases. This could compensate – at least for a period of a few days – for the decline in photosynthesis (and hence isoprene precursors).

Leaf-level isoprene emission (I) in Arneth et al. (2007b) is given by:

$$I_l = IEF \frac{A_J + R_D}{(A_J)_{st} + R_{D,st}} f_T \cdot f_{CO_2} \quad (6)$$

$$f_T = \text{MIN} [\exp(a_t(T - T_{st})); 2.3] \quad (7)$$

where T is air temperature and the “st” subscript indicates that the variable is measured under standard conditions (see Eq. 5). The empirical factor a_T is set to 0.1 and accounts for the higher temperature optimum of isoprene synthesis compared to that of the electron transport rate. Although isoprene is produced in the chloroplast from precursors formed during photosynthesis, there are differences in the short-term response of carbon assimilation and isoprene emission, such as the higher temperature optimum of isoprene synthase (Monson et al., 1992). IEF is the basal isoprene emission at the leaf level under standard conditions. Isoprene is not stored in the leaf (Sanadze, 2004) and therefore emitted isoprene reflects the instantaneous rate of synthesis.

2.3 Coupling of the isoprene emission scheme into JULES

The structure of JULES required a modification of the original Arneth et al. (2007b) scheme because electron transport is not explicitly simulated in the JULES photosynthesis scheme. We assume that the rate of net photosynthesis is a reasonable approximation to the electron transport dependent rate of net photosynthesis, and simulate above-canopy isoprene emission (I) as:

$$I = IEF \frac{A + R_D}{A_{st} + R_{D,st}} f_T \cdot f_{CO_2} \cdot LAI \quad (8)$$

Evaluation of a photosynthesis-based biogenic isoprene emission

F. Pacifico et al.

Title Page

Abstract

Introduction

Conclusions

References

Tables

Figures

⏪

⏩

◀

▶

Back

Close

Full Screen / Esc

Printer-friendly Version

Interactive Discussion



where Leaf Area Index (LAI) defined as the canopy leaf area per unit ground area is used to scale up emissions from leaf to canopy level and is updated to the phenological status of the vegetation type.

Equation (8) describes the strong relationship between isoprene production and photosynthesis (Delwiche and Sharkey, 1993), but also takes into account the CO_2 inhibition (f_{CO_2}) and the fact that temperature optimum for photosynthesis is lower than for isoprene synthesis (f_T).

2.4 Evaluation strategy against ground-based isoprene flux measurements

Ground-based measurements of above-canopy isoprene fluxes, with temporal resolution and length of measurements sufficient for our purpose are only available from 6 sites (see Table 1). These sites are located in broadleaf forests, specifically temperate deciduous broadleaf forest and tropical rain forest (Table 1). Measurements have generally been made for a relatively short period within the growing season when the leaves are mature; only the record from the University of Michigan Biological Station (UMBS; Pressley et al., 2005) covers more than one year. We used the available data from all of the flux tower sites to evaluate the diurnal cycle and daily variability in isoprene emission. The UMBS site has been used to evaluate the seasonal cycle during 2000 and 2002, while the Harvard forest site has been used to evaluate the 1995 seasonal cycle. Data acquisition problems delayed the start of measurements at the UMBS site in 2001 until after the onset of isoprene emissions and measurements were not continued until the end of the growing season. We therefore cannot use the data from 2001 to evaluate the seasonal cycle of isoprene emissions.

We simulate isoprene emissions at each flux site using the single-point version of JULES. We used locally measured IEFs at La Verdière and Montmeyan sites (Dominique Serça, unpublished data); when local IEFs were not available, we used standard IEF values for the appropriate vegetation type derived from Guenther et al. (1995): $45 \mu\text{gC gdw}^{-1} \text{h}^{-1}$ for temperate deciduous broadleaf forest and $24 \mu\text{gC gdw}^{-1} \text{h}^{-1}$ for tropical rain forest. The meteorological data used to run JULES were either

Evaluation of a photosynthesis-based biogenic isoprene emission

F. Pacifico et al.

Title Page

Abstract

Introduction

Conclusions

References

Tables

Figures

⏪

⏩

◀

▶

Back

Close

Full Screen / Esc

Printer-friendly Version

Interactive Discussion



Evaluation of a photosynthesis-based biogenic isoprene emission

F. Pacifico et al.

[Title Page](#)[Abstract](#)[Introduction](#)[Conclusions](#)[References](#)[Tables](#)[Figures](#)[⏪](#)[⏩](#)[◀](#)[▶](#)[Back](#)[Close](#)[Full Screen / Esc](#)[Printer-friendly Version](#)[Interactive Discussion](#)

measurements made on-site (UMBS, Harvard Forest, Manaus and Santarem km 67) or were derived from nearby meteorological stations (data from Puechabon 43.7° N, 3.6° E were used for La Verdière and Montmeyan). Although isoprene fluxes were generally only measured for short periods, meteorological observations were collected for longer (at least two years). However, meteorological data were not available at the hourly time step on which the model was run. It was therefore necessary to fill these observational gaps. Since the gaps were typically several days long interpolation was not feasible. Instead missing observations were replaced by the average values of that time step from other years. For example, if data for 11:00 a.m. on the 24 April was missing in one year, then we used the average value for this time step in previous years. This method maintains the diurnal- and seasonal-cycle of each variable at the expense of reduced variance. The gap-filling technique was not applied to rainfall or snowfall rates because it would potentially lead to erroneous introduction of small-scale precipitation events (from the averaging across years). The gap-filled values were compared with the actual observations at the site, when available, and in no case did this procedure introduce a radical departure from the observed variable changes through the day. The number of data points averaged for gap filling depends mainly on the site (the more years of data the more years available for averaging). The proportion of gap-filled temperature and radiation data was always less than 10% of the available data.

We quantified how well the model reproduces the magnitude, diurnal and day-to-day variability of the observations using linear correlation of hourly emissions, daily average emissions and daily maximum emissions. We also evaluated the simulated seasonal cycle of isoprene emissions against observations from the UMBS and the Harvard forest sites. The correlations were calculated only for the hours when observations were made at each site.

2.5 Evaluation strategy against satellite derived estimates

Satellite observations of formaldehyde (HCHO) have been used to estimate biogenic isoprene emissions at a regional and global scale (e.g., Shim et al., 2005; Palmer et al., 2003, 2006; Fu et al., 2007; Barkley et al., 2008, 2009). In this study, we use HCHO-derived isoprene estimates over east and south Asia between 1996 and 2001 (Fu et al., 2007) and tropical South America between 1997 and 2001 (Barkley et al., 2008). We focus on tropical regions for evaluation against satellite-derived data because of the assumed importance of tropical areas as an isoprene source (Guenther et al., 2006), and because the two tropical flux-tower sites only provide short-term measurements and thus there is no other source of data about changes over the seasonal cycle at the tropics. We have selected satellite-derived isoprene estimates where the potential contribution of biomass burning to HCHO has been constrained: Fu et al. (2007) used local reports of annual burning along with satellite fire counts, while Barkley et al. (2008) used Along Track Scanning Radiometer (ATSR) fire counts and GOME NO₂ columns to estimate the impact of biomass burning on HCHO. For east and south Asia in summer, Fu et al. (2007) found that the interference to isoprene estimates due to HCHO produced by anthropogenic VOC is small. Both studies use the Global Ozone Monitoring Experiment (GOME) satellite observations of HCHO and the GEOS-Chem chemistry transport model. The east and south Asia data set provides an average annual emission based on the period 1996 and 2001. The tropical South America data set records monthly mean isoprene emissions at the satellite overpass time (i.e. between 10:00 to 12:00 a.m. local time). Both data sets can be used to evaluate spatial patterns and the magnitude of total isoprene emissions; but only the South America data set can be used to evaluate the seasonal cycle and year-to-year variability of emissions. The errors associated with estimating emissions from remotely-sensed HCHO are typically of the order 100% and predominately originate from errors in (a) the HCHO slant column retrieval, (b) the air-mass factor calculation (which converts the slant to a vertical column) and (c) uncertainties in the simplified representation of isoprene oxidation

Evaluation of a photosynthesis-based biogenic isoprene emission

F. Pacifico et al.

Title Page

Abstract

Introduction

Conclusions

References

Tables

Figures



Back

Close

Full Screen / Esc

Printer-friendly Version

Interactive Discussion



chemistry within the chemistry transport model (CTM; Barkley et al., 2008). Although the uncertainties of these estimates are large they are nevertheless still comparable to the uncertainties of estimates derived from an inventory approach.

For comparison with the satellite-based estimates of isoprene emission, we ran the model globally at half-degree resolution with a 1 h time step from 1990 to 2001 using meteorological inputs from the Integrated Project Water and Global Change (WATCH) Forcing Data (WFD; Weeton et al., 2010) and 360 ppm CO₂ atmospheric concentration. The WFD data are available at half-degree resolution over land (excluding Antarctica). However, downward longwave radiation, air pressure, specific humidity, air temperature, and wind speed are only provided at 6-hourly time steps, together with code to allow variable-specific interpolation to 3-hourly time steps and downward shortwave radiation, rainfall and snowfall are only provided at 3-hourly time steps. The data were therefore interpolated to the 1-hour timestep required by the model. The distribution of PFTs in this simulation is based on the International Geosphere-Biosphere Programm (IGBP) dataset (Loveland et al., 2000). The 17 land cover classes in this dataset were translated into proportional cover and characteristics of the five JULES PFTs and the proportional cover of the four JULES land cover types according to Table 2 and 3. PFT distribution is kept fixed over the simulated time period. IEFs values were derived from Guenther et al. (1995) and are: 35 $\mu\text{gC gdw}^{-1} \text{h}^{-1}$ for broadleaf trees; 12 $\mu\text{gC gdw}^{-1} \text{h}^{-1}$ for needleleaf trees; 16 $\mu\text{gC gdw}^{-1} \text{h}^{-1}$ for C3 grass; 8 $\mu\text{gC gdw}^{-1} \text{h}^{-1}$ for C4 grass and; 20 $\mu\text{gC gdw}^{-1} \text{h}^{-1}$ for shrubs. We extracted the simulated emissions for the same areas and spatial resolutions as in the satellite-derived emission estimates. We compared simulated against satellite-derived isoprene emissions in magnitude and spatial variability, seasonal and inter-annual variability are also evaluated when available. We only consider emissions over land as our scheme focuses on isoprene emission and does not include simulation of lateral transport.

Evaluation of a photosynthesis-based biogenic isoprene emission

F. Pacifico et al.

[Title Page](#)[Abstract](#)[Introduction](#)[Conclusions](#)[References](#)[Tables](#)[Figures](#)[Back](#)[Close](#)[Full Screen / Esc](#)[Printer-friendly Version](#)[Interactive Discussion](#)

2.6 Protocol for modern global simulation

We have estimated global isoprene emissions from 1990 to 1999 based on the global simulation described above. These estimates are compared with previous model-derived estimates from the literature.

3 Results

3.1 Model evaluation against ground-based isoprene flux measurements

Simulated total daily isoprene emissions are always higher than observations (Table 4). When applying the generic IEF from Guenther et al. (1995), the model overestimates the total daily isoprene emissions by a maximum of 150% at La Verdière. The use of a locally measured IEF instead of the generic IEF improves the magnitude of simulated emissions at La Verdière, but it has only a small impact on the magnitude of isoprene emissions at Montmeyan, where locally measured IEF and generic IEF are more similar to each other than at La Verdière (Table 1).

The coupled model generally reproduces the trend of the observed diurnal cycle of isoprene emissions (Fig. 1). In addition, the model correctly reproduces the onset of emissions, except at Manaus where modelled emissions start 1 h (1 time step in the model) after observed emissions. Simulated emissions continue for 1 h (1 time step in the model) after observed emissions cease. The time of peak emission is correctly simulated at the UMBS site, but is delayed by between 1 (e.g., see Montmeyan in Fig. 1) and 3 hours (e.g., see Manaus in Fig. 1) at the other sites. The magnitude of emissions during the early part of the day is correctly simulated, but simulated emissions in the middle of the day and in the afternoons are generally higher than observed.

The model overestimates observed hourly emissions when using the generic IEFs at all sites except at the Harvard forest (Fig. 2). The UMBS and the La Verdière sites are the best simulated in terms of hourly emissions, using the generic IEF and the

**Evaluation of a
photosynthesis-
based biogenic
isoprene emission**

F. Pacifico et al.

Title Page

Abstract

Introduction

Conclusions

References

Tables

Figures

⏪

⏩

◀

▶

Back

Close

Full Screen / Esc

Printer-friendly Version

Interactive Discussion



locally-derived IEF respectively. Hourly emissions are less well simulated at the Manaus and the Santarem sites, where we previously observed that simulated emissions are generally too high in the middle of the day and in the afternoons (Fig. 1). Correlation coefficients for hourly emissions are between 0.44 and 0.69 (all values significant at 95% level) across the sites (Fig. 2).

The model generally overestimates daily average emissions at all sites (Fig. 3). The UMBS and the Harvard forest sites are the best simulated in terms of daily average emissions and are also the bigger data sets (Fig. 3). The correlation coefficients for daily average emissions at each site vary between 0.33 and 0.84 (all significant at the 95% level, except those at La Verdière) across the sites (Fig. 3).

The model overestimates daily maximum emissions at the Manaus and the Santarem sites (Fig. 4), where we previously observed too high simulated peak emissions (Fig. 1). The use of locally-derived IEF significantly improves the magnitude of simulated peak emissions at La Verdière (Fig. 4). The correlation coefficients for daily maximum emissions vary between 0.06 and 0.80 (all significant at the 95% level, except those at La Verdière and Manaus) across all sites (Fig. 4).

Both the observations and simulations at the UMBS site (Fig. 5) show a similar seasonal pattern, with emissions starting in May, increasing rapidly through May and June and reaching their maximum values during June, July and August. The onset of emissions is less well simulated in 2000 than in 2002, when simulated emissions start ca. 20 days earlier than observed, albeit at a very low rate. The model reproduces the observed decline in emissions during the autumn but simulated emissions continue for 20–30 days longer than shown by the observations. This reflects the fact that simulated LAI is still high during the autumn (Fig. 5), with simulated leaf fall beginning up to 30 days later than observed (Pressley et al., 2005). Despite the bigger number of missing data for the observations compared to the UMBS data set, similar results are found for the Harvard forest site: the model reproduces the observed seasonal cycle in magnitude, but it shows a longer seasonal cycle with simulated emissions starting too early in spring and continuing too long over autumn (not shown here).

3.2 Model evaluation against satellite derived estimates

Satellite-derived total annual mean isoprene emissions over east and south Asia (12° S–55° N, 70° E–150° E) averaged over the years 1996–2001 have been estimated as 50 TgC yr⁻¹, with an uncertainty of 26 TgC (Fu et al., 2007), compared to a simulated value of 58 TgC on average over the 6 year simulation period (standard deviation: 2 TgC). The satellite-derived spatial distribution of the emissions over east and south Asia shows a gradient from low emissions in the north-west, which is mostly deserts and mountains, to high emissions in the south and east (Fig. 6). This pattern is also apparent in the simulation but with a larger gradient (Fig. 6). The model reproduces the generally low emissions over India and the higher emissions over Indochina. Simulated emissions over Indonesia and Papua are higher than observed. The model produces lower emissions in northern China and into eastern Siberia than shown in the satellite-derived product.

Satellite-derived area-weighted total isoprene emissions over tropical South America are 24.3 gC m⁻² (standard deviation: 0.6 gC m⁻²) compared to a simulated value of 26.7 gC m⁻² (standard deviation: 0.3 gC m⁻²). The trend of the simulated seasonal cycle over tropical South America is similar to the observed trend, but of higher magnitude (Fig. 7). Modelled emissions are generally higher than satellite-derived ones in May and in part of the dry season as well, especially November. The month of May coincides with the transition from the wet to the dry period, which is when an unusual drop in isoprene emissions has been potentially attributed to leaf flushing (Barkley et al., 2009). Inter-annual variability is larger in the satellite-derived estimates, which are derived from generally noisy HCHO satellite data (Barkley et al., 2008).

Spatial variability of isoprene emissions over tropical South America is broadly reproduced except for some observed peak values and generally slightly higher modelled emissions over the north-eastern coast (see e.g. Fig. 8 for year 1999). Inter-annual spatial variability is larger in the satellite-derived estimates, which are also noisier. Correlation coefficients for month-to-month variability are between 0.83 and 0.95 (all values significant at 95% level; data not shown).

Evaluation of a photosynthesis-based biogenic isoprene emission

F. Pacifico et al.

Title Page

Abstract

Introduction

Conclusions

References

Tables

Figures



Back

Close

Full Screen / Esc

Printer-friendly Version

Interactive Discussion



3.3 Isoprene emission global estimates

Published estimates of annual global total isoprene emissions for present-day (based on different time periods between 1971 to 2003) range from 400 to 600 TgC yr⁻¹, with an average over the different studies of 516 TgC yr⁻¹ (see Table 1 in Arneth et al., 2008a). Our annual global total estimate ranges between 368 and 394 TgC yr⁻¹, with 380 TgC yr⁻¹ averaged over the period 1990 to 1999; this is lower than the estimate obtained by Sanderson et al. (2003) for the same decade (483 TgC yr⁻¹) and lower than other estimates for modern climate conditions (see Table 1 in Arneth et al., 2008a). In our simulation, the greatest contribution to modelled global isoprene emissions is given by broadleaf trees (245 TgC, 64%), followed by C3 grass (46 TgC, 12%), C4 grass (43 TgC, 11%), needleleaf trees (30 TgC, 8%) and shrubs (16 TgC, 4%). Broadleaf trees are also the most abundant PFT in JULES vegetation distribution maps (Fig. 10).

The results from Arneth et al. (2007a) and Guenther et al. (2006) are based on different time periods from that covered by our simulation but can be used to compare the first-order patterns of emissions. As in our simulation, both Arneth et al. (2007a) and Guenther et al. (2006) show the tropics as main source of isoprene (Fig. 9). We simulate a smaller magnitude of emissions over central and South America, central Africa, Indochina and some European areas than Arneth et al. (2007a) and less spatial variability over Amazonia. We also simulate less isoprene emissions over Australia than in Guenther et al. (2006).

One of the greatest uncertainties in modelling the global emission of isoprene is the use of generic PFT-dependent IEFs. We have calculated the IEFs we would need to use to achieve 600 TgC yr⁻¹ without further changes in the model (see Table 5). These emission factors are within the observed range of species-level IEFs measurements (Hewitt and Street, 1992; Wiedinmyer et al., 2004) for each of the model PFTs.

Inter-annual variability of global total isoprene emissions is correlated with global temperature anomalies (Fig. 11). The 1992 minimum in isoprene emissions is associated with reduced radiation and cooler and drier conditions following Mt. Pinatubo

Evaluation of a photosynthesis-based biogenic isoprene emission

F. Pacifico et al.

Title Page

Abstract

Introduction

Conclusions

References

Tables

Figures



Back

Close

Full Screen / Esc

Printer-friendly Version

Interactive Discussion



month longer than observed. Our ability to simulate the seasonal cycle of isoprene emissions, and hence the magnitude of the yearly emissions, is critically dependent on the phenology of individual PFTs as simulated by JULES. Improvements to, for example, the controls of leaf fall in JULES could produce a significant improvement in our estimates of isoprene emissions.

A limited number of measurements have shown that young leaves do not emit isoprene (Centritto et al., 2004) and there is a typical lag of a few weeks between the onset of photosynthesis and that of isoprene emissions (e.g., Wiberley et al., 2005). We do not take leaf age into consideration in the isoprene emission scheme, although this would be possible. Our limited evaluation of the onset of emissions at the UMBS and the Harvard forest sites does not provide any guidance as to whether such a treatment is necessary: we simulate the onset of isoprene emission in 2002 and fail to simulate it in 2000. However, the lack of this mechanism in our simulations could be a possible explanation for the mismatch between modelled and satellite-derived isoprene emissions in the transition from the wet to the dry period over tropical South America. The model overestimates isoprene emissions in the dry season over tropical South America compared to satellite-derived isoprene estimates. This could be due to the fact that the model does not have explicit representation of agricultural crops, but uses the frequently applied C3 herbaceous vegetation PFT as a surrogate (e.g., Bondeau et al., 2007). While both C3 grasses and crop vegetation have low isoprene emission potential, there is also distinct difference in seasonality, with crops often harvested before the end of the growing season. Other possible causes for this could be linked to environmental effects on isoprene emission not included in the model, such as leaf age as well as leaf “brown-down” owing to prolonged dryness (Huete et al., 2006).

We have shown that using locally-derived IEFs instead of generic IEFs from Guenther et al. (1995) produced a better simulation of emissions in magnitude at one flux measurement sites (La Verdière), but yielded only a slight improvement in the other site where a locally measured IEF is available (Montmeyan). In gap-models like LPJ-GUESS that (at least for some regions) resolve actual tree species by their plant

Evaluation of a photosynthesis-based biogenic isoprene emission

F. Pacifico et al.

Title Page

Abstract

Introduction

Conclusions

References

Tables

Figures



Back

Close

Full Screen / Esc

Printer-friendly Version

Interactive Discussion



**Evaluation of a
photosynthesis-
based biogenic
isoprene emission**

F. Pacifico et al.

Title Page

Abstract

Introduction

Conclusions

References

Tables

Figures



Back

Close

Full Screen / Esc

Printer-friendly Version

Interactive Discussion

functional type parameterisations and description of canopy structural and growth dynamics, the use of species-specific emission factors has been shown to provide an important asset for isoprene simulations (Arneth et al., 2008a; Schurgers et al., 2009). The vegetation representation in JULES is much more generic, and at the regional scale (as shown by the comparisons with the HCHO-derived emissions) the model is able to reproduce the main features of isoprene spatial variability and magnitude using the more general PFT-dependent IEFs from Guenther et al. (1995). This implies that the use of average values for IEFs is a reasonable approximation for global modelling.

In our simulation broadleaf trees are the major contributors to total global emissions because they are the most abundant PFT in vegetation distribution maps (Fig. 10), they have the highest IEF and they are widely present in tropical areas where temperature and light conditions favour isoprene emissions. Despite their relatively high IEF, shrubs contribute little to total global emissions because of their smaller coverage in the PFT distribution map used to drive the simulations (Fig. 10).

We simulate slightly higher than observed isoprene emissions for our two regional case studies but our global total estimate of isoprene emissions is lower than previously published estimates. We identify the tropics as the main source of isoprene, as do previous estimates (Arneth et al., 2007a; Guenther et al., 2006), but we generally simulate less isoprene emissions over tropical areas and less spatial variability in emissions. The absence of isoprene “emission hotspots” in our simulations may explain the lower levels of tropical emissions. This, in turn, is likely to be related to the relatively simple PFT classification used in JULES. Where other models include both raingreen and evergreen broadleaf tropical trees (e.g. Arneth et al., 2007a), JULES has only one type of broadleaf tree in the tropics. However, our estimation of global total isoprene emissions is still within the uncertainties on PFT-dependent IEFs (Table 5). The large uncertainty on PFT-dependent IEFs implies that increasing the number of simulated PFTs in JULES would not make a large difference in the estimation of global isoprene emissions.

**Evaluation of a
photosynthesis-
based biogenic
isoprene emission**

F. Pacifico et al.

Title Page

Abstract

Introduction

Conclusions

References

Tables

Figures



Back

Close

Full Screen / Esc

Printer-friendly Version

Interactive Discussion



Most of the isoprene emission flux measurements have been collected in tree-dominated biomes, as they are considered the main emitters (Guenther et al., 2006). Nevertheless observations collected in an Inner Mongolia grassland reach values comparable to a tree-dominated environment (Bai et al., 2006), while summer-time maxima in a sub-arctic Swedish wetland could reach values similar to boreal and temperate forest locations (Holst et al., 2008). We have been unable to make a simulation for these sites because of the lack of local meteorological data; in particular downward longwave and shortwave radiation were not available for a time period long enough to perform a local simulation. Our global simulations driven by the WATCH re-analysis meteorological data did not show any notable isoprene emissions over these areas. This might be due to the fact that in the global simulation we use generic IEFs that are not representative of the measurement site.

Our ability to evaluate the isoprene emission schemes is somewhat hampered by lack of data. There are very few above-canopy isoprene flux measurements available, and the existing studies sample a limited range of vegetation types. Additional studies on a range of different biomes and with measurements made for longer periods are necessary. Robust evaluation of model performance requires measurements over multiple years in order to validate the simulated seasonal cycle and to determine whether it is important to simulate the impact of leaf aging on isoprene emissions explicitly. Nevertheless, the current evaluation provides increased confidence in our ability to simulate isoprene emissions realistically at the global scale, and hence opens up the possibility of exploring and quantifying the feedbacks between biogenic emissions and climate more fully (e.g., Arneth et al., 2010), both in the context of studies of air quality and future climate change (e.g., Young et al., 2009) as well as for palaeoclimates (e.g., Valdes et al., 2005).

Acknowledgements. This paper is a contribution to the GREENCYCLES (MRTN-CT-2004-512464) (FP, SPH, SS). This work has been partly funded by EUCAARI (European Integrated project on Aerosol Cloud Climate and Air Quality interactions) No 036833-2. FP, CJ and GPW were supported by the Joint DECC/Defra Met Office Hadley Centre Climate

Programme (GA01101). MPB was supported by the Natural Environment Research Council (grant NE/D001471). AA and GS acknowledge support by the Swedish Research Councils Vetenskapsrådet and Formas. We thank Shelley Pressley for use of the UMBS isoprene flux measurements and Thomas Karl for the use of the Manaus isoprene flux measurements.
5 We thank Lina Mercado, David Pearson, Emma Compton, Gerd Folberth, Doug McNeill and Richard Betts for their help.

References

- Arneth, A., Miller, P. A., Scholze, M., Hickler, T., Schurgers, G., Smith, B., and Prentice, I. C.: CO₂ inhibition of global terrestrial isoprene emissions: potential implications for atmospheric chemistry, *Geophys. Res. Lett.*, 34, L18813, doi:10.1029/2007GL030615, 2007a.
- 10 Arneth, A., Niinemets, Ü., Pressley, S., Bäck, J., Hari, P., Karl, T., Noe, S., Prentice, I. C., Serça, D., Hickler, T., Wolf, A., and Smith, B.: Process-based estimates of terrestrial ecosystem isoprene emissions: incorporating the effects of a direct CO₂-isoprene interaction, *Atmos. Chem. Phys.*, 7, 31–53, doi:10.5194/acp-7-31-2007, 2007b.
- 15 Arneth, A., Monson, R. K., Schurgers, G., Niinemets, Ü., and Palmer, P. I.: Why are estimates of global terrestrial isoprene emissions so similar (and why is this not so for monoterpenes)?, *Atmos. Chem. Phys.*, 8, 4605–4620, doi:10.5194/acp-8-4605-2008, 2008a.
- Arneth, A., Schurgers, G., Hickler, T., and Miller, P. A.: Effects of species composition, land surface cover, CO₂ concentration and climate on isoprene emissions from European forests, *Plant Biology*, 9, 1–12, 2008b.
- 20 Arneth, A., Sitch, S., Bondeau, A., Butterbach-Bahl, K., Foster, P., Gedney, N., de Noblet-Ducoudré, N., Prentice, I. C., Sanderson, M., Thonicke, K., Wania, R., and Zaehle, S.: From biota to chemistry and climate: towards a comprehensive description of trace gas exchange between the biosphere and atmosphere, *Biogeosciences*, 7, 121–149, doi:10.5194/bg-7-121-2010, 2010.
- 25 Bai, J., Baker, B., Liang, B., Greenberg, J., and Guenther, A.: Isoprene and monoterpene emissions from an Inner Mongolia grassland, *Atmos. Environ.*, 40, 5753–5758, 2006.
- Barkley, M. P., Palmer, P. I., Kuhn, U., Kesselmeier, J., Chance, K., Kurosu, T. P., Martin, R. V., Helmig, D., and Guenther, A.: Net ecosystem fluxes of isoprene over tropical South America

Evaluation of a photosynthesis-based biogenic isoprene emission

F. Pacifico et al.

Title Page

Abstract

Introduction

Conclusions

References

Tables

Figures

⏪

⏩

◀

▶

Back

Close

Full Screen / Esc

Printer-friendly Version

Interactive Discussion



Evaluation of a photosynthesis-based biogenic isoprene emission

F. Pacifico et al.

Title Page

Abstract

Introduction

Conclusions

References

Tables

Figures

⏪

⏩

◀

▶

Back

Close

Full Screen / Esc

Printer-friendly Version

Interactive Discussion

- inferred from Global Ozone Monitoring Experiment (GOME) observations of HCHO columns, *J. Geophys. Res.*, 113, D20304, doi:10.1029/2008JD009863, 2008.
- Barkley, M. P., Palmer, P. I., De Smedt, I., Karl, T., Guenther, A., and Van Roozendaal, M.: Regulated large-scale annual shutdown of Amazonian isoprene emissions?, *Geophys. Res. Lett.*, 36, L04803, doi:10.1029/2008GL036843, 2009.
- Blyth, E., Clark, D. B., Ellis, R., Huntingford, C., Los, S., Pryor, M., Best, M., and Sitch, S.: A comprehensive set of benchmark tests for a land surface model of simultaneous fluxes of water and carbon at both the global and seasonal scale, *Geosci. Model Dev. Discuss.*, 3, 1829–1859, doi:10.5194/gmdd-3-1829-2010, 2010a.
- Blyth, E., Gash, J., Lloyd, A., Pryor, M., Weedon, G. P., and Shuttleworth, W. J.: Evaluating the JULES land surface model energy fluxes using FLUXNET data, *J. Hydrometeorol.*, 11, 509–519, 2010b.
- Bondeau, A., Smith, P. C., Zaehle, S., Schaphoff, S., Lucht, W., Cramer, W., Gerten, D., Lotze-Camper, H., Müller C., Reichstein, M., and Smith, B.: Modelling the role of agriculture for the 20th century global terrestrial carbon balance, *Glob. Change Biol.*, 13(3), 679–706, 2007.
- Brohan, P., Kennedy, J. J., Harris, I., Tett, S. F. B., and Jones, P. D.: Uncertainty estimates in regional and global observed temperature changes: a new dataset from 1850, *J. Geophys. Res.*, 111, D12106, doi:10.1029/2005JD006548, 2006.
- Cadule, P., Friedlingstein, P., Bopp, L., Sitch, S., Jones, C. D., Ciais, P., Piao, S. L., and Peylin, P.: Benchmarking coupled climate-carbon models against long-term atmospheric CO₂ measurements, *Global Biogeochem. Cy.*, 24, GB2016, doi:10.1029/2009GB003556, 2010.
- Centritto, M., Nascetti, P., Petrilli, L., Raschi, A., and Loreto, F.: Profiles of isoprene emission and photosynthetic parameters in hybrid poplars exposed to free-air CO₂ enrichment, *Plant Cell Environ.*, 27, 403–412, 2004.
- Claeys, M., Graham, B., Vas, G., Wang, W., Vermeylen, R., Pashynska, V., Cafmeyer, J., Guyon, P., Andreae, M. O., Artaxo, P., and Maenhaut, W.: Formation of secondary organic aerosols through photooxidation of isoprene, *Science*, 303, 1173–1176, 2004.
- Collatz, G. J., Ball, J. T., Grivet, C., and Berry, J. A.: Physiological and environmental regulation of stomatal conductance, photosynthesis and transpiration: A model that includes a laminar boundary layer, *Agr. Forest Meteorol.*, 54, 107–136, 1991.
- Collatz, G. J., Ribas-Carbo, M., and Berry, J. A.: A coupled photosynthesis- stomatal conductance model for leaves of C4 plants, *Aust. J. Plant Physiol.*, 19, 519–538, 1992.
- Cox, P. M., Huntingford, C., and Harding, R. J.: A canopy conductance and photosynthesis

Evaluation of a photosynthesis-based biogenic isoprene emission

F. Pacifico et al.

[Title Page](#)

[Abstract](#)

[Introduction](#)

[Conclusions](#)

[References](#)

[Tables](#)

[Figures](#)

[⏪](#)

[⏩](#)

[◀](#)

[▶](#)

[Back](#)

[Close](#)

[Full Screen / Esc](#)

[Printer-friendly Version](#)

[Interactive Discussion](#)



model for use in a GCM land surface scheme, *J. Hydrol.*, 213, 79–94, 1998.

Cox, P. M., Betts, R., Bunton, C. B., Essery, R. L. H., Rowtree, P. R., and Smith, J.: The impact of new land surface physics on the GCM simulation of climate and climate sensitivity, *Clim. Dynam.*, 15, 183–203, 1999.

5 Cox, P., M., Betts, R. A., Jones, C. D., Spall, S. A., and Totterdell, I. J.: Acceleration of global warming due to carbon-cycle feedbacks in a coupled climate model, *Nature*, 408, 184–187, 2000.

Cox, P. M.: Description of the "TRIFFID" Dynamic Global Vegetation Model. Technical note 24, Met Office Hadley Centre, Exeter, UK, 17 pp., 2001.

10 Delwiche, C. F. and Sharkey, T. D.: Rapid appearance of ^{13}C in biogenic isoprene when $^{13}\text{CO}_2$ is fed into intact leaves, *Plant Cell Environ.*, 16, 587–591, 1993.

Essery, R. L. H., Best, M. J., Betts, R. A., Cox, P. M., and Taylor, C. M.: Explicit Representation of Subgrid Heterogeneity in a GCM Land Surface Scheme, *J. Hydrometeorol.*, 4, 530–543, 2003.

15 Farquhar, G. D., Caemmerer, S., and Berry, J. A.: A biochemical model of photosynthetic CO_2 assimilation in leaves of C3 species, *Planta*, 149, 78–90, 1980.

Fu, T., Jacob, D. J., Palmer, P. I., Chance, K., Wang, Y. X., Barletta, B., Blake, D. R., Stanton, J. C., and Pilling, M. J.: Space-based formaldehyde measurements as constraints on volatile organic compound emissions in east and south Asia and implications for ozone, *J. Geophys. Res.*, 112, D06312, doi:10.1029/2006JD007853, 2007.

20 Goldstein, A. H., Goulden, M. L., Munger, J. W., Wofsy, S. C., and Geron, C. D.: Seasonal course of isoprene emissions from a midlatitude deciduous forest, *J. Geophys. Res.*, 103(D23), 31045–31056, 1998.

25 Guenther, A. B., Monson, R. K., and Fall, R.: Isoprene and monoterpene emission rate variability: observations with eucalyptus and emission rate algorithm development, *J. Geophys. Res.*, 96, 10799–10808, 1991.

Guenther, A. B., Zimmerman, P. R., Harley, P. C., Monson, R. K., and Fall, R.: Isoprene and monoterpene emission rate variability – model evaluations and sensitivity analyses, *J. Geophys. Res.*, 98(D7), 12609–12617, 1993.

30 Guenther, A., Hewitt, C. N., Erickson, D., Fall, R., Geron, C., Graedel, T., Harley, P., Klinger, L., Lerdau, M., McKay, W. A., Pierce, T., Scholes, B., Steinbrecher, R., Tallamraju, R., Taylor, J., and Zimmerman, P.: A global model of natural volatile organic compound emissions, *J. Geophys. Res.*, 100(D5), 8873–8892, 1995.

**Evaluation of a
photosynthesis-
based biogenic
isoprene emission**

F. Pacifico et al.

Title Page

Abstract

Introduction

Conclusions

References

Tables

Figures

◀

▶

◀

▶

Back

Close

Full Screen / Esc

Printer-friendly Version

Interactive Discussion



- Guenther, A.: The contribution of reactive carbon emissions from vegetation to the carbon balance of terrestrial ecosystems, *Chemosphere*, 49, 837–844, 2002.
- Guenther, A., Karl, T., Harley, P., Wiedinmyer, C., Palmer, P. I., and Geron, C.: Estimates of global terrestrial isoprene emissions using MEGAN (Model of Emissions of Gases and Aerosols from Nature), *Atmos. Chem. Phys.*, 6, 3181–3210, doi:10.5194/acp-6-3181-2006, 2006.
- Harley, P. C., Monson, R. K., and Lerdau, M. T.: Ecological and evolutionary aspects of isoprene emission from plants, *Oecologia*, 118, 109–123, 1999.
- Hewitt, C. N. and Street, R. A.: A qualitative assessment of the emission of nonmethane hydrocarbon compounds from the biosphere to the atmosphere in the UK: present knowledge and uncertainties, *Atmos. Environ.*, 26A(17), 3069–3077, 1992.
- Hofzumahaus, A., Rohrer, F., Lu, K., Bohn, B., Brauers, T., Chang, C.-C., Fuchs, H., Holland, F., Kita, K., Kondo, Y., Li, X., Lou, S., Shao, M., Zeng, L., Wahner, A., and Zhang, Y.: Amplified trace gas removal in the troposphere, *Science*, 324, 1702–1704, 2009.
- Holst, T., Arneeth, A., Hayward, S., Ekberg, A., Mastepanov, M., Jackowicz-Korczynski, M., Friborg, T., Crill, P. M., and Bäckstrand, K.: BVOC ecosystem flux measurements at a high latitude wetland site, *Atmos. Chem. Phys.*, 10, 1617–1634, doi:10.5194/acp-10-1617-2010, 2010.
- Huete, A. R., Didan, K., Shimabukuro, Y. E., Ratana, P., Saleska, S. R., Hutyra, L. R., Yang, W., Nemani, R. R., and Myneni, R.: Amazon rainforests green-up with sunlight in dry season, *Geophys. Res. Lett.*, 33, L06405, doi:10.1029/2005GL025583, 2006.
- Johns, T. C., Durman, C. F., Banks, H. T., et al.: The new Hadley Centre climate model HadGEM1: Evaluation of coupled simulations, *J. Climate*, 19, 1327–1353, 2006.
- Karl, T., Guenther, A., Yokelson, R. J., Greenberg, J., Potosnak, M., Blake, D. R., and Artaxo, P.: The tropical forest and fire emissions experiment: emission, chemistry, and transport of biogenic volatile organic compounds in the lower atmosphere over Amazonia, *J. Geophys. Res.*, 112, D18302, doi:10.1029/2007JD008539, 2007.
- Kesselmeier, J. and Staudt M.: Biogenic volatile organic compounds (VOC): An overview on emission, physiology and ecology, *J. Atmos. Chem.*, 33, 23–88, 1999.
- Loveland, T. R., Reed, B. C., Brown, J. F., Ohlen, D. O., Zhu, Z., Yang, L., and Merchant, J. W.: Development of a global land cover characteristics database and IGBP DISCover from 1 km AVHRR data, *Int. J. Remote Sens.*, 21(6–7), 1303–1330, 2000.
- Martin, M. J., Stirling, C. M., Humphries, S. W., and Long, S. P.: A process-based model to

Evaluation of a photosynthesis-based biogenic isoprene emission

F. Pacifico et al.

Title Page

Abstract

Introduction

Conclusions

References

Tables

Figures

⏪

⏩

◀

▶

Back

Close

Full Screen / Esc

Printer-friendly Version

Interactive Discussion



predict the effects of climatic change on leaf isoprene emission rates, *Ecol. Model.*, 131, 161–174, 2000.

Mercado, L. M., Huntingford, C., Gash, J. H. C., Cox, P. M., and Jogireddy, V.: Improving the representation of radiation interception and photosynthesis for climate model applications, *Tellus B*, 59, 553–565, 2007.

Monson, R. K. and Fall, R.: Isoprene emission from aspen leaves, *Plant Physiol.*, 90, 267–274, 1989.

Monson, R. K., Jaeger, C. H., Adams, W. W., Driggers, E. M., Silver, G. M., and Fall, R.: Relationships among isoprene emission rate, photosynthesis, and isoprene synthase activity as influenced by temperature, *Plant Physiol.*, 98, 1175–1180, 1992.

Monson, R. K., Trahan, N., Rosenstiel, T. N., Veres, P., Moore, D., Wilkinson, M., Norby, R. J., Volder, A., Tjoelker, M. G., Briske, D. D., Karnosky, D. F., and Fall, R.: Isoprene emission from terrestrial ecosystems in response to global change: minding the gap between models and observations, *Philos. T. R. Soc. A.*, 365, 1677–1695, 2007.

Müller, J.-F., Stavrou, T., Wallens, S., De Smedt, I., Van Roozendael, M., Potosnak, M. J., Rinne, J., Munger, B., Goldstein, A., and Guenther, A. B.: Global isoprene emissions estimated using MEGAN, ECMWF analyses and a detailed canopy environment model, *Atmos. Chem. Phys.*, 8, 1329–1341, doi:10.5194/acp-8-1329-2008, 2008.

Niinemets, Ü., Tenhunen, J. D., Harley, P. C., and Steinbrecher, R.: A model of isoprene emission based on energetic requirements for isoprene synthesis and leaf photosynthetic properties for *Liquidambar* and *Quercus*, *Plant Cell Environ.*, 22, 1319–1335, 1999.

Niinemets, Ü., Arneth, A., Kuhn, U., Monson, R. K., Peñuelas, J., and Staudt, M.: The emission factor of volatile isoprenoids: stress, acclimation, and developmental responses, *Biogeosciences*, 7, 2203–2223, doi:10.5194/bg-7-2203-2010, 2010a.

Niinemets, Ü., Monson, R. K., Arneth, A., Ciccioli, P., Kesselmeier, J., Kuhn, U., Noe, S. M., Peñuelas, J., and Staudt, M.: The leaf-level emission factor of volatile isoprenoids: caveats, model algorithms, response shapes and scaling, *Biogeosciences*, 7, 1809–1832, doi:10.5194/bg-7-1809-2010, 2010b.

Pacifico, F., Harrison, S. P., Jones, C. D., and Sitch, S.: Isoprene emissions and climate, *Atmos. Environ.*, 43(39), 6121–6135, 2009.

Palmer, P. I., Jacob, D. J., Fiore, A. M., Martin, R. V., Chance, K., and Kurosu, T. P.: Mapping isoprene emissions over North America using formaldehyde column observations from space, *J. Geophys. Res.*, 108(D6), 4180, doi:10.1029/2002JD002153, 2003.

Evaluation of a photosynthesis-based biogenic isoprene emission

F. Pacifico et al.

Title Page

Abstract

Introduction

Conclusions

References

Tables

Figures

⏪

⏩

◀

▶

Back

Close

Full Screen / Esc

Printer-friendly Version

Interactive Discussion



- Palmer, P. I., Abbot, D. S., Fu, T.-M., Jacob, D. J., Chance, K., Kurosu, T. P., Guenther, A., Wiedinmyer, C., Stanton, J. C., Pilling, M. J., Pressley, S. N., Lamb, B., and Sumner, A. L.: Quantifying the seasonal and interannual variability of North American isoprene emissions using satellite observations of the formaldehyde column, *J. Geophys. Res.*, 111, D12315, doi:10.1029/2005JD006689, 2006.
- 5 Pegoraro, E., Rey, A., Bobich, E. G., Barron-Gafford, G., Grieve, K. A., Malhi, Y., and Murthy, R.: Effect of elevated CO₂ concentration and vapour pressure deficit on isoprene emission from leaves of *Populus deltoides* during drought, *Funct. Plant Biol.*, 31, 1137–1147, 2004.
- Pressley, S., Lamb, B., Westberg, H., Flaherty, J., Chen, J., and Vogel, C.: Long-term isoprene flux measurements above a northern hardwood forest, *J. Geophys. Res.*, 110, D07301, doi:10.1029/2004JD005523, 2005.
- 10 Rosenstiel, T. N., Ebbets, A. L., Khatri, W. C., Fall, R., and Monson, R. K.: Induction of Poplar leaf nitrate reductase: A test of extrachloroplastic control of Isoprene emission rate, *Plant Biol.*, 6, 12–21, 2004.
- 15 Sanadze, G. A.: Biogenic isoprene (a review), *Russ. J. Plant Physiol.*, 51(6), 729–741, 2004.
- Sanderson, M. G., Jones, C. D., Collins, W. J., Johnson, C. E., and Derwent, R. G.: Effect of climate change on isoprene emissions and surface ozone levels, *Geophys. Res. Lett.*, 30(18), 1936 pp., 2003.
- Sellers, P. J., Berry, J. A., Collatz, G. J., Field, C. B., and Hall, F. G.: Canopy reflectance, photosynthesis, and transpiration III. A reanalysis using improved leaf models and a new canopy integration scheme, *Remote Sens. Environ.*, 42, 187–216, 1992.
- 20 Sharkey, T. D. and Loreto, F.: Water stress, temperature, and light effects on the capacity for isoprene emission and photosynthesis of kudzu leaves, *Oecologia*, 95, 328–333, 1993.
- Shim, C., Wang, Y., Choi, Y., Palmer, P. I., Abbot, D., and Chance, K.: Constraining global isoprene emissions with Global Ozone Monitoring Experiment (GOME) formaldehyde column measurements, *J. Geophys. Res.*, 110, D24301, doi:10.1029/2004JD005629, 2005.
- 25 Schurgers, G., Hickler, T., Miller, P. A., and Arneth, A.: European emissions of isoprene and monoterpenes from the Last Glacial Maximum to present, *Biogeosciences*, 6, 2779–2797, doi:10.5194/bg-6-2779-2009, 2009.
- 30 Sitch, S., Smith, B., Prentice, I. C., Arneth, A., Bondeau, A., Cramer, W., Kaplan, J. O., Levis, S., Lucht, W., Sykes, M. T., Thonicke, K., and Venevsky, S.: Evaluation of ecosystem dynamics, plant geography and terrestrial carbon cycling in the LPJ dynamic global vegetation model, *Glob. Change Biol.*, 9(2), 161–185, 2003.

**Evaluation of a
photosynthesis-
based biogenic
isoprene emission**

F. Pacifico et al.

[Title Page](#)[Abstract](#)[Introduction](#)[Conclusions](#)[References](#)[Tables](#)[Figures](#)[⏪](#)[⏩](#)[◀](#)[▶](#)[Back](#)[Close](#)[Full Screen / Esc](#)[Printer-friendly Version](#)[Interactive Discussion](#)

Smith, B., Prentice, I. C., and Sykes, M. T.: Representation of vegetation dynamics in the modelling of terrestrial ecosystems: comparing two contrasting approaches within European climate space, *Global Ecol. Biogeogr.*, 10, 621–637, 2001.

Telford, P. J., Lathi re, J., Abraham, N. L., Archibald, A. T., Braesicke, P., Johnson, C. E., Morgenstern, O., O'Connor, F. M., Pike, R. C., Wild, O., Young, P. J., Beerling, D. J., Hewitt, C. N., and Pyle, J.: Effects of climate-induced changes in isoprene emissions after the eruption of Mount Pinatubo, *Atmos. Chem. Phys.*, 10, 7117–7125, doi:10.5194/acp-10-7117-2010, 2010.

Valdes, P. J., Beerling, D. J., and Johnson, C. E.: The ice age methane budget, *Geophys. Res. Lett.*, 32, L02704, doi:10.1029/2004GL021004, 2005.

Weedon, G. P., Gomes, S., Viterbo, P.,  sterle, H., Adam, J. C., Bellouin, N., Boucher, O., and Best, M.: The WATCH forcing data 1958–2001: a meteorological forcing dataset for land surface and hydrological models. WATCH technical report 22, available at: www.eu-watch.org, 2010.

Wiberley, A. E., Linskey, A. R., Falbel, T. G., and Sharkey, T. D.: Development of the capacity for isoprene emission in kudzu, *Plant Cell Environ.*, 28(7), 898–905, 2005.

Wiedinmyer, C., Guenther, A., Harley, P., Hewitt, C. N., Geron, C., Artaxo, P., Steinbrecher, R., and Rasmussen, R.: Global organic emissions from vegetation, in: *Emissions of Atmospheric Trace Compounds*, edited by: Granier, C., Artaxo, P., and Reeves, C. E, Kluwer Publishing Co, Dordrecht, The Netherlands, 115–170, 2004.

Wolter, K. and Timlin, M.: Monitoring ENSO in COADS with a seasonally adjusted principal component index, in: *Proc. of the 17th Climate Diagnostics Workshop*, Norman, OK, NOAA/N MC/CAC, NSSL, Oklahoma Clim. Survey, CIMMS and the School of Meteor., Univ. of Oklahoma, 52–57, 1993.

Wolter, K. and Timlin, M. S.: Measuring the strength of ENSO events – how does 1997/98 rank? *Weather*, 53, 315–324, 1998.

Young, P. J., Arneith, A., Schurgers, G., Zeng, G., and Pyle, J. A.: The CO₂ inhibition of terrestrial isoprene emission significantly affects future ozone projections, *Atmos. Chem. Phys.*, 9, 2793–2803, doi:10.5194/acp-9-2793-2009, 2009.

Zimmer, W., Steinbrecher, R., K rner, C., and Schnitzler, J.-P.: The process-based SIM-BIM model: towards more realistic prediction of isoprene emissions from adult *Quercus petraea* forest trees, *Atmos. Environ.*, 37(12), 1665–1671, 2003.

Table 1. Description of ground-based isoprene flux tower sites.

Site and Location	Record Period	Biome	JULES PFT	Dominant Species	Local IEF ($\mu\text{gC gdw}^{-1} \text{h}^{-1}$)	IEF from Guenther et al. (1995) ($\mu\text{gC gdw}^{-1} \text{h}^{-1}$)	CO ₂ atmospheric concentration used in JULES (ppm)	References
University of Michigan Biological Station (UMBS), USA 45.5° N, 84.7° W	May 2000 to October 2002 (~5 months every year)	Temperate deciduous broadleaf forest	Broadleaf trees	<i>Populus grandidentata</i> , <i>P. tremuloides</i> , <i>Fagus grandifolia</i> , <i>Betula papyrifera</i> , <i>Acer rubrum</i> , <i>A. saccharum</i> , <i>Quercus rubra</i> , <i>Pinus strobus</i> , <i>Pteridium aquilium</i>		45	369	Pressley et al. (2005)
Harvard Forest, Massachusetts, USA 42.5° N, 72.2° W	May to November 1995 (160 days)	Temperate deciduous broadleaf forest	Broadleaf trees	<i>Quercus rubra</i> , <i>Acer rubrum</i> , <i>Pinus strobus</i> , <i>Betula lenta</i> , <i>Tsuga canadensis</i> , <i>Castanea dentata</i>		45	360	Goldstein et al. (1998), Müller et al. (2008)
La Verdrière, France 43.6° N, 6.0° E	June–July 2000 (~14 days)	Temperate deciduous broadleaf forest	Broadleaf trees	<i>Quercus pubescens</i> ,	24.2	45	368	Dominique Serça, unpublished data
Montmeyan, France 43.6° N, 6.1° E	June 2001 (~13 days)	Temperate deciduous broadleaf forest	Broadleaf trees	<i>Quercus pubescens</i>	37.2	45	369	Dominique Serça, unpublished data
60 km NNW of Manaus, Brazil 2.6° S, 60.2° W	September 2004 (~9 days)	Tropical rain forest	Broadleaf trees			24	376	Karl et al. (2007)
Santarem 67 km, Brazil 2.9° S, 55.0° W	October–November 2003 (15 days)	Tropical rain forest	Broadleaf trees			24	375	Müller et al. (2008)

Evaluation of a photosynthesis-based biogenic isoprene emission

F. Pacifico et al.

Title Page

Abstract

Introduction

Conclusions

References

Tables

Figures

◀

▶

◀

▶

Back

Close

Full Screen / Esc

Printer-friendly Version

Interactive Discussion



Evaluation of a photosynthesis-based biogenic isoprene emission

F. Pacifico et al.

Title Page

Abstract

Introduction

Conclusions

References

Tables

Figures

⏪

⏩

◀

▶

Back

Close

Full Screen / Esc

Printer-friendly Version

Interactive Discussion



Table 2. Conversion of IGBP land cover classes into JULES fractions of surface types.

IGBP description	Fractions of JULES surface types								
	Broadleaf trees	Needleleaf trees	C3 grass	C4 grass	Shrubs	Urban	Water Soil	Bare	Ice
Evergreen Needleleaf Forest	0.0	69.3	22.2	0.0	0.0	0.0	0.0	8.4	0.0
Evergreen Broadleaf Forest	85.9	0.0	0.9	7.0	0.0	0.0	0.0	6.2	0.0
Deciduous Needleleaf Forest	0.0	65.3	25.6	0.0	0.0	0.0	0.0	9.1	0.0
Deciduous Broadleaf Forest	62.4	0.0	7.0	8.9	3.7	0.0	0.0	18.1	0.0
Mixed Forest	35.5	35.5	20.9	0.0	0.0	0.0	0.0	8.2	0.0
Closed Shrubs	0.0	0.0	25.0	0.0	60.0	0.0	0.0	15.0	0.0
Open Shrubs	0.9	0.0	3.1	14.7	34.2	0.0	0.0	47.2	0.0
Woody Savannah	50.0	0.0	15.0	0.0	25.0	0.0	0.0	10.0	0.0
Savannah	20.0	0.0	0.0	75.0	0.0	0.0	0.0	5.0	0.0
Grassland	0.0	0.0	66.0	15.7	4.9	0.0	0.0	13.5	0.0
Permanent Wetland	2.2	0.0	80.9	0.0	1.4	0.0	15.0	0.6	0.0
Cropland	0.1	0.0	66.0	3.4	0.2	0.0	0.0	20.4	0.0
Urban	0.0	0.0	0.0	0.0	0.0	100.0	0.0	0.0	0.0
Crop/Natural Mosaic	5.0	5.0	55.0	15.0	10.0	0.0	0.0	10.0	0.0
Snow and Ice	0.0	0.0	0.0	0.0	0.0	0.0	0.0	0.0	100.0
Barren	0.0	0.0	0.0	0.0	0.0	0.0	0.0	100.0	0.0
Water Bodies	0.0	0.0	0.0	0.0	0.0	0.0	100.0	0.0	0.0

Evaluation of a photosynthesis-based biogenic isoprene emission

F. Pacifico et al.

Title Page

Abstract

Introduction

Conclusions

References

Tables

Figures

◀

▶

◀

▶

Back

Close

Full Screen / Esc

Printer-friendly Version

Interactive Discussion



Table 3. Conversion of IGBP LAI into LAI for JULES PFTs.

IGBP description	Leaf area index of JULES plant functional types				
	Broadleaf trees	Needleleaf trees	C3 grass	C4 grass	Shrubs
Evergreen Needleleaf Forest		6	2		
Evergreen Broadleaf Forest	9		2	4	
Deciduous Needleleaf Forest		4	2		
Deciduous Broadleaf Forest	5		2	4	3
Mixed Forest	5	6	2		
Closed Shrubs			2		3
Open Shrubs	5		2	4	2
Woody Savannah	9		4		2
Savannah	9			4	
Grassland			3	4	3
Permanent Wetland	9		3		3
Cropland	5		5	4	3
Crop/Natural Mosaic	5	6	4	4	3

Evaluation of a photosynthesis-based biogenic isoprene emission

F. Pacifico et al.

Table 4. Observed and simulated average total diurnal budget of isoprene emissions at the flux tower sites listed in Table 1.

Site	Observed average total diurnal budget of isoprene emissions ($\text{mgC m}^{-2} \text{ day}^{-1}$)	Simulated average total diurnal budget of isoprene emissions with local IEFs ($\text{mgC m}^{-2} \text{ day}^{-1}$)	Simulated average total diurnal budget of isoprene emissions with IEFs from Guenther et al. (1995) ($\text{mgC m}^{-2} \text{ day}^{-1}$)
UMBS	29		44
Harvard Forest	30		36
La Verdière	28	42	70
Montmeyan	57	80	87
Manaus	34		69
Santarem	21		44

Title Page

Abstract

Introduction

Conclusions

References

Tables

Figures

⏪

⏩

◀

▶

Back

Close

Full Screen / Esc

Printer-friendly Version

Interactive Discussion



Evaluation of a photosynthesis-based biogenic isoprene emission

F. Pacifico et al.

Title Page

Abstract

Introduction

Conclusions

References

Tables

Figures

⏪

⏩

◀

▶

Back

Close

Full Screen / Esc

Printer-friendly Version

Interactive Discussion



Table 5. Sensitivity of total annual emissions to the specification of PFT-specific IEFs.

PFTs	IEFs ($\mu\text{gC gdw}^{-1} \text{h}^{-1}$) used in this study	Total global annual isoprene emissions averaged over the 1990s (TgC yr^{-1})	IEFs ($\mu\text{gC gdw}^{-1} \text{h}^{-1}$) needed to achieve total global annual isoprene emissions of 600 TgC yr^{-1}
Broadleaf trees	35	245 (64%)	55
Needleleaf trees	12	30 (8%)	19
C3 grass	16	46 (12%)	25
C4 grass	8	43 (11%)	13
Shrubs	20	16 (4%)	32
Total over PFTs		380	

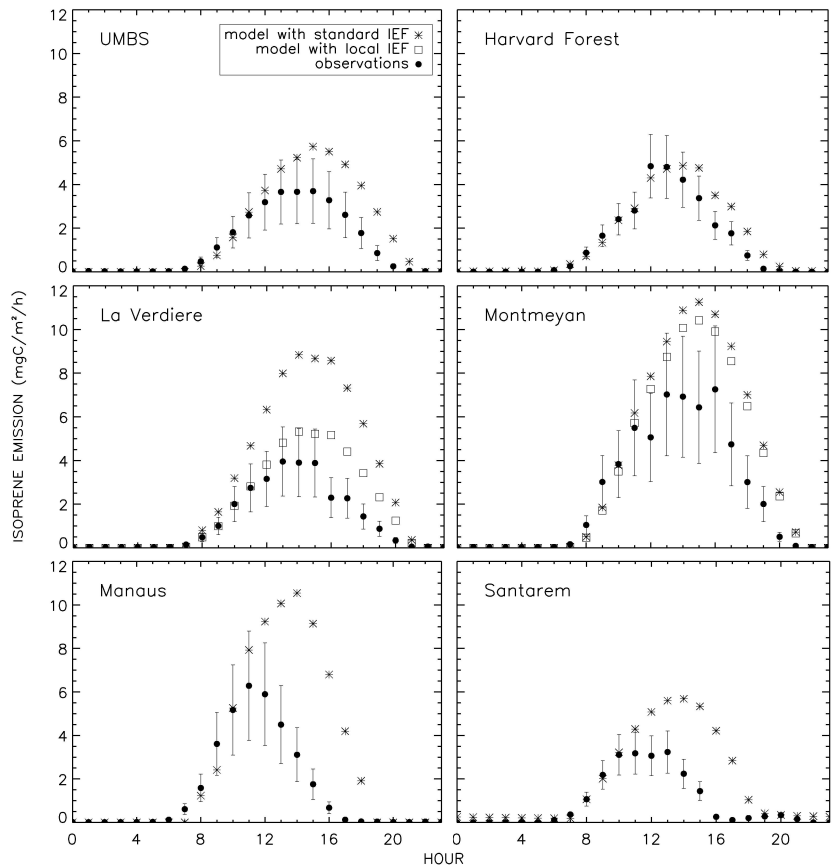


Fig. 1. Comparison of simulated and ground-based measured mean diurnal cycles of isoprene emissions at the flux tower sites listed in Table 1. Isoprene emissions were simulated using standard IEFs from Guenther et al. (1995) and local IEFs when available.

Evaluation of a photosynthesis-based biogenic isoprene emission

F. Pacifico et al.

Title Page

Abstract Introduction

Conclusions References

Tables Figures

◀ ▶

◀ ▶

Back Close

Full Screen / Esc

Printer-friendly Version

Interactive Discussion



Evaluation of a photosynthesis-based biogenic isoprene emission

F. Pacifico et al.

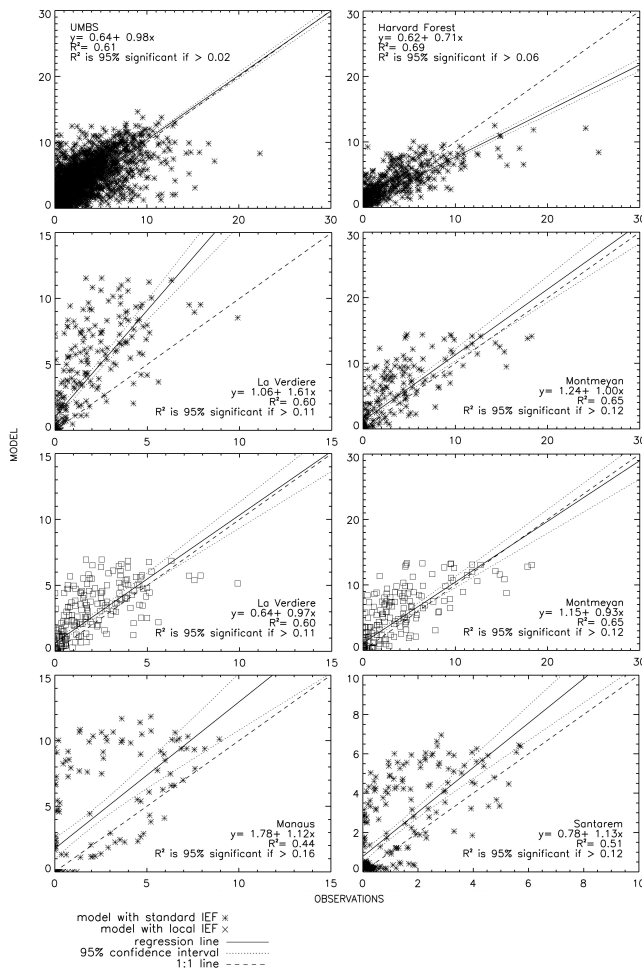


Fig. 2. Scatter plots of simulated and ground-based measured hourly isoprene emissions at the flux tower sites listed in Table 1, including regression line, 95% confidence interval (Scheffe’s method) and 1:1 line. Isoprene emissions were simulated using standard isoprene emission factors (IEFs) from Guenther et al. (1995) and local IEFs when available.

Title Page

Abstract Introduction

Conclusions References

Tables Figures

◀ ▶

◀ ▶

Back Close

Full Screen / Esc

Printer-friendly Version

Interactive Discussion



Evaluation of a photosynthesis-based biogenic isoprene emission

F. Pacifico et al.

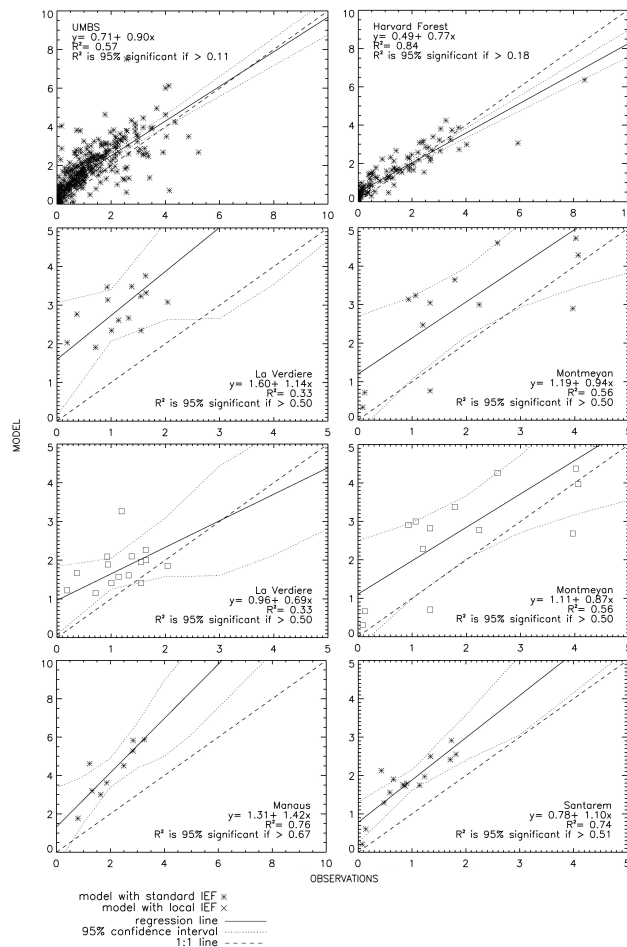


Fig. 3. Scatter plots of simulated and ground-based measured daily average isoprene emissions at the flux tower sites listed in Table 1, including regression line, 95% confidence interval (Scheffe's method) and 1:1 line. Isoprene emissions were simulated using standard isoprene emission factors (IEFs) from Guenther et al. (1995) and local IEFs when available.

Title Page

Abstract Introduction

Conclusions References

Tables Figures

◀ ▶

◀ ▶

Back Close

Full Screen / Esc

Printer-friendly Version

Interactive Discussion



Evaluation of a photosynthesis-based biogenic isoprene emission

F. Pacifico et al.

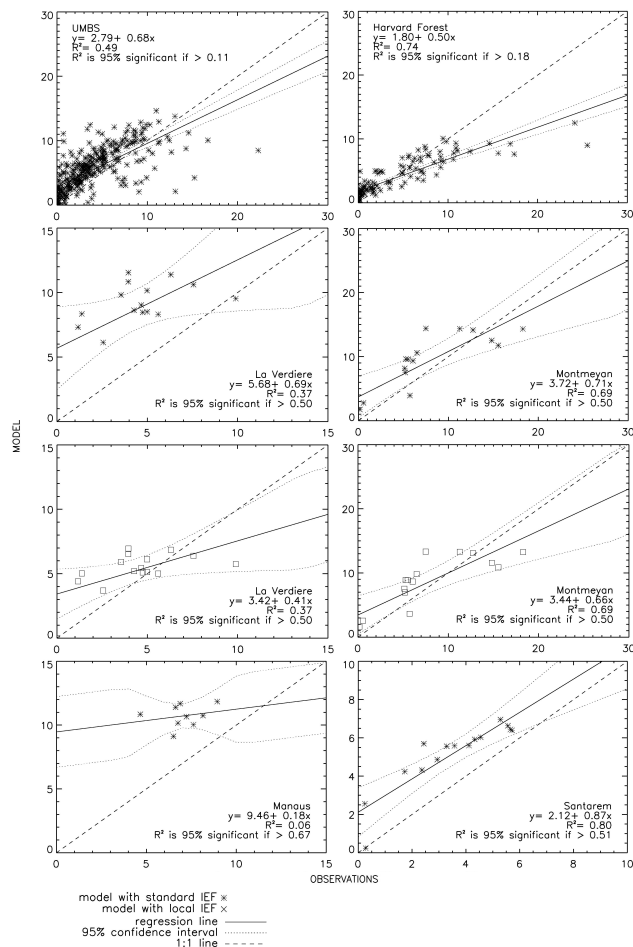


Fig. 4. Scatter plots of simulated and ground-based measured daily maximum isoprene emissions at the flux tower sites listed in Table 1, including regression line, 95% confidence interval (Scheffe's method) and 1:1 line. Isoprene emissions were simulated using standard isoprene emission factors (IEFs) from Guenther et al. (1995) and local IEFs when available.

Title Page

Abstract Introduction

Conclusions References

Tables Figures

◀ ▶

◀ ▶

Back Close

Full Screen / Esc

Printer-friendly Version

Interactive Discussion



**Evaluation of a
photosynthesis-
based biogenic
isoprene emission**

F. Pacifico et al.

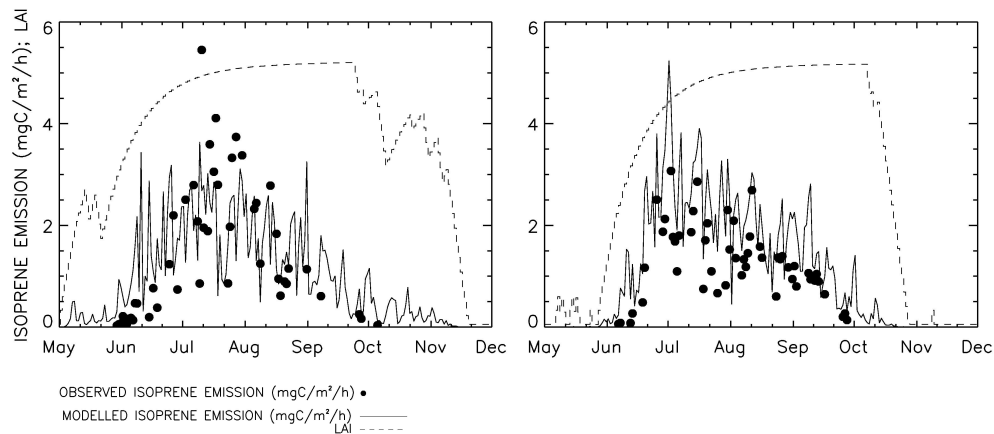


Fig. 5. Comparison of simulated and ground-based measured seasonal cycle of daily mean isoprene emissions, and simulated LAI at UMBS for 2000 and 2002.

[Title Page](#)[Abstract](#)[Introduction](#)[Conclusions](#)[References](#)[Tables](#)[Figures](#)[◀](#)[▶](#)[◀](#)[▶](#)[Back](#)[Close](#)[Full Screen / Esc](#)[Printer-friendly Version](#)[Interactive Discussion](#)

**Evaluation of a
photosynthesis-
based biogenic
isoprene emission**

F. Pacifico et al.

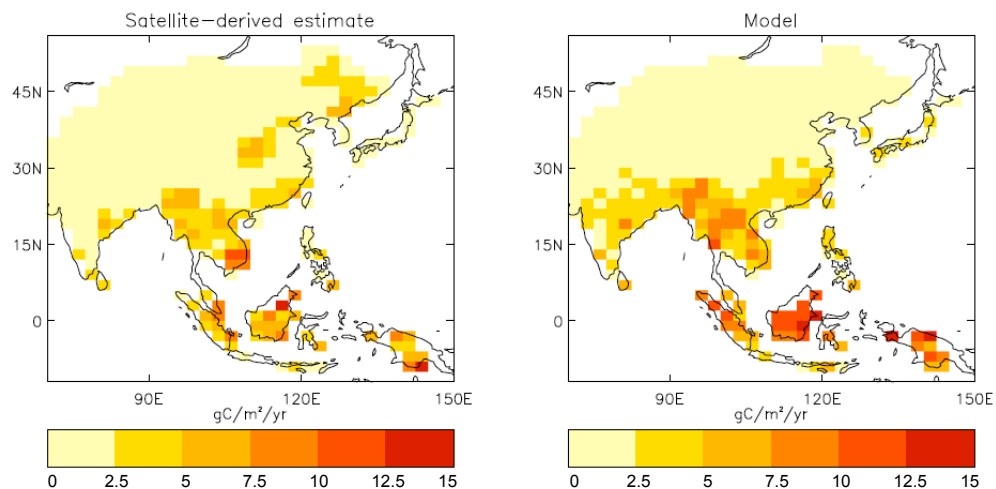


Fig. 6. Comparison of spatial patterns of simulated and satellite-derived total annual isoprene emissions over east and south Asia averaged over 1996 to 2001.

[Title Page](#)[Abstract](#)[Introduction](#)[Conclusions](#)[References](#)[Tables](#)[Figures](#)[⏪](#)[⏩](#)[◀](#)[▶](#)[Back](#)[Close](#)[Full Screen / Esc](#)[Printer-friendly Version](#)[Interactive Discussion](#)

Evaluation of a photosynthesis-based biogenic isoprene emission

F. Pacifico et al.

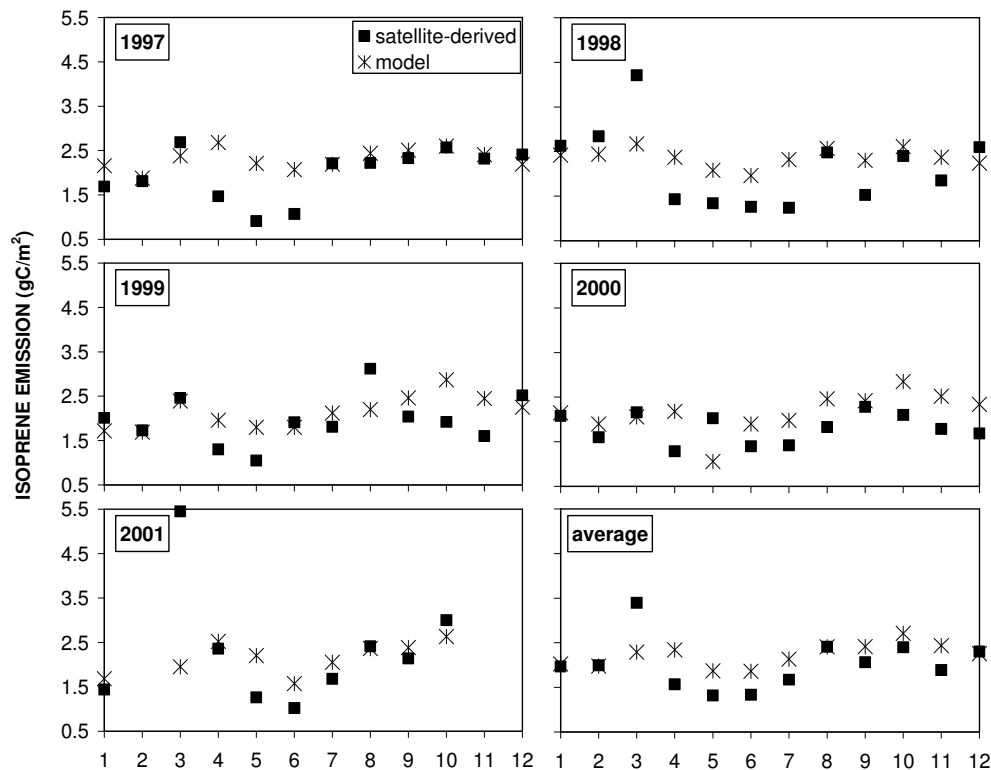


Fig. 7. Comparison of simulated and satellite-derived monthly total isoprene emissions (10–12 LT) over tropical South America for individual years from 1997 to 2001, May to November.

[Title Page](#)
[Abstract](#)
[Introduction](#)
[Conclusions](#)
[References](#)
[Tables](#)
[Figures](#)
[⏪](#)
[⏩](#)
[◀](#)
[▶](#)
[Back](#)
[Close](#)
[Full Screen / Esc](#)
[Printer-friendly Version](#)
[Interactive Discussion](#)

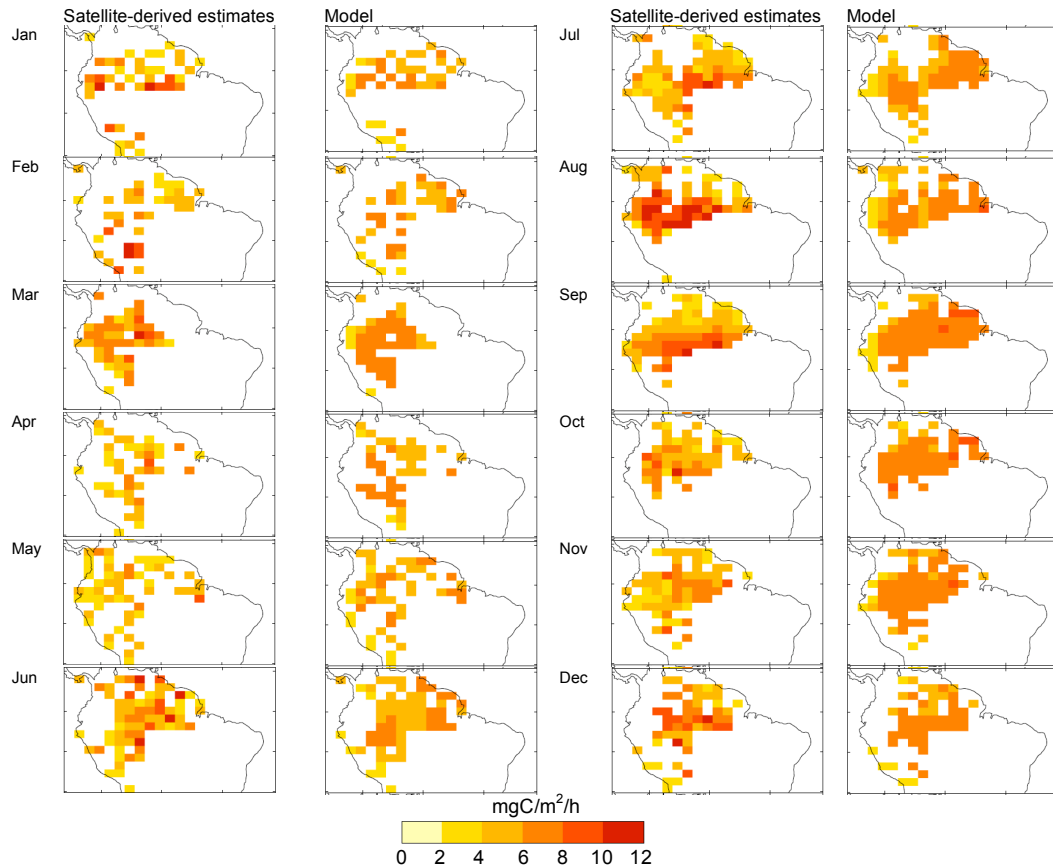


Fig. 8. Comparison of spatial patterns of simulated and satellite-derived monthly mean isoprene emissions (10–12 LT) over tropical South America for 1999.

Evaluation of a photosynthesis-based biogenic isoprene emission

F. Pacifico et al.

Title Page

Abstract Introduction

Conclusions References

Tables Figures

⏪ ⏩

◀ ▶

Back Close

Full Screen / Esc

Printer-friendly Version

Interactive Discussion



**Evaluation of a
photosynthesis-
based biogenic
isoprene emission**

F. Pacifico et al.

Title Page

Abstract

Introduction

Conclusions

References

Tables

Figures

◀

▶

◀

▶

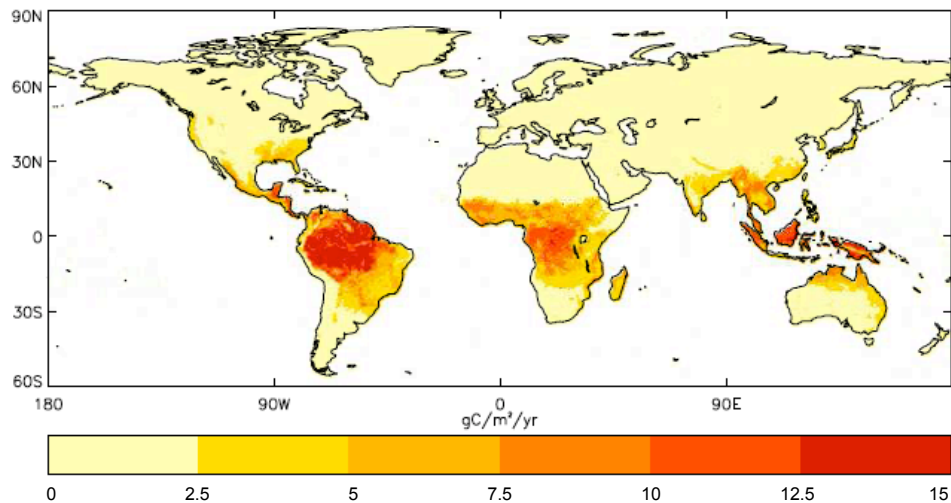
Back

Close

Full Screen / Esc

Printer-friendly Version

Interactive Discussion

**Fig. 9.** Annual global simulation of isoprene emissions averaged over the 1990s.

**Evaluation of a
photosynthesis-
based biogenic
isoprene emission**

F. Pacifico et al.

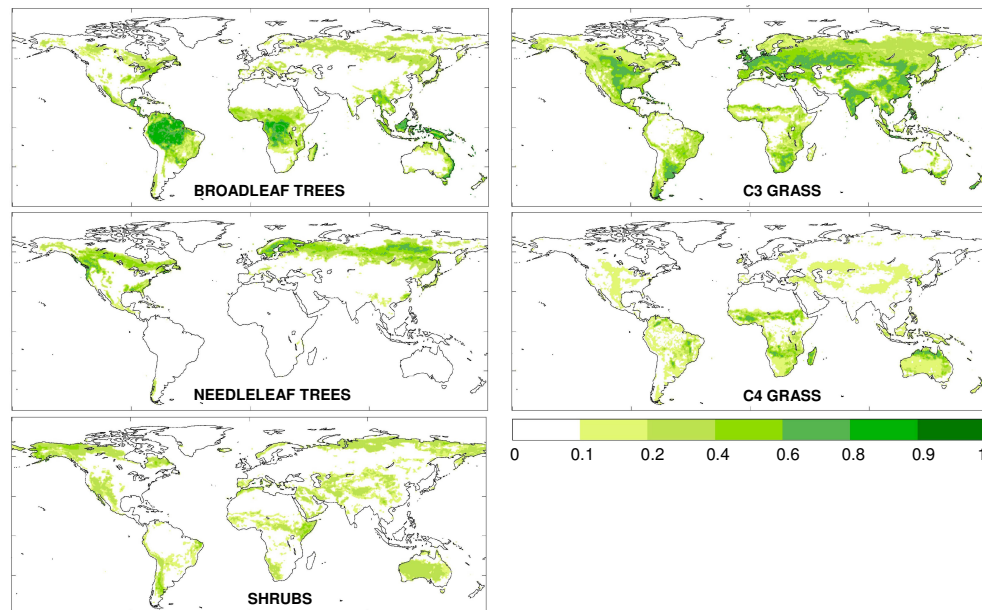


Fig. 10. Maps of the fraction of grid cell covered by each PFT as used in JULES.

[Title Page](#)[Abstract](#)[Introduction](#)[Conclusions](#)[References](#)[Tables](#)[Figures](#)[⏪](#)[⏩](#)[◀](#)[▶](#)[Back](#)[Close](#)[Full Screen / Esc](#)[Printer-friendly Version](#)[Interactive Discussion](#)

Evaluation of a photosynthesis-based biogenic isoprene emission

F. Pacifico et al.

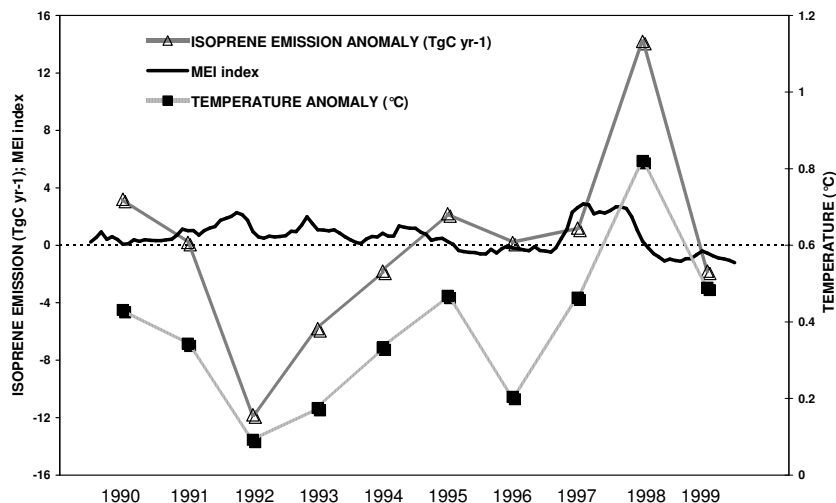


Fig. 11. Inter-annual variability of simulated global total isoprene emissions anomalies, global average land air temperature anomalies from the historical surface temperature dataset CRUTEM3 (Brohan et al., 2006) and Multivariate El Niño/Southern Oscillation (ENSO) Index (MEI; Wolter and Timlin, 1993, 1998) over the 1990s.

Title Page

Abstract

Introduction

Conclusions

References

Tables

Figures

◀

▶

◀

▶

Back

Close

Full Screen / Esc

Printer-friendly Version

Interactive Discussion

